Hyperfine Magnetic Substate Resolved State-to-State Chemistry

Joschka Wolf⊙, Markus Deiß, and Johannes Hecker Denschlag

Institut für Quantenmaterie and Center for Integrated Quantum Science and Technology IQST,
Universität Ulm, 89069 Ulm, Germany

We extend state-to-state chemistry to a realm where besides vibrational, rotational, and hyperfine quantum states magnetic quantum numbers are also resolved. For this, we make use of the Zeeman effect, which energetically splits levels of different magnetic quantum numbers. The chemical reaction which we choose to study is three-body recombination in an ultracold quantum gas of ^{87}Rb atoms forming weakly bound Rb$_2$ molecules. Here, we find the propensity rule that the total m_F quantum number of the two atoms forming the molecule is conserved. Our method can be employed for many other reactions and inelastic collisions and will allow for novel insights into few-body processes.

A primary goal of state-to-state chemistry is to gain an understanding about chemical reactions on a fundamental level (see, e.g., [1]). This includes investigating what the final product states are for a given quantum state of reactants. A proven experimental method for carrying out state-to-state chemistry is based on atomic and molecular beams (for recent reviews, see, e.g., [2–5]). In recent years, a complementary approach has been established, investigating chemical reactions in traps in the ultracold regime (for reviews, see [6–11]).

Within the last decades it has become standard for state-to-state chemistry experiments to resolve the electronic, vibrational, and rotational quantum states of the molecular reactants and products. This includes in particular the alignment or orientation of the molecules, corresponding to a control of the magnetic quantum number of rotation, which is important for investigating stereodynamical aspects (see, e.g., [12–17]). Very recently our group demonstrated that even hyperfine states of the products can be resolved [18,19]. The general detection of their magnetic substates, however, has still been missing. Only in special cases where the inelastic process is taking place in a single quantum channel was it possible to identify the hyperfine quantum number. Typical examples for single-channel dominated reactions occur in the vicinity of Feshbach resonances, e.g., [20–24], or are photoinduced reactions, e.g., [25,26].

Clearly, state-to-state aspects become especially of interest when more than one reaction channel is involved. Here, we extend state-to-state chemistry to finally resolve hyperfine magnetic substates for systems where many reaction channels are present. This is achieved by measuring how the molecular product states are Zeeman shifted as a function of an applied external magnetic field. The chemical reaction which we choose to study is three-body recombination of ^{87}Rb where two atoms combine to form a

Rb$_2$ dimer and the third Rb atom (spectator) carries away part of the released binding energy, see Fig. 1(a). We work at low magnetic fields of a few G where atomic interactions are nonresonant [18,19]. We probe molecular quantum states in a range of small binding energies and find the following "no-spin flip" propensity rule. The m_F quantum number of the molecule equals the sum of the initially prepared m_f quantum numbers of the two atoms which form the molecule. Here, m_F is the magnetic quantum
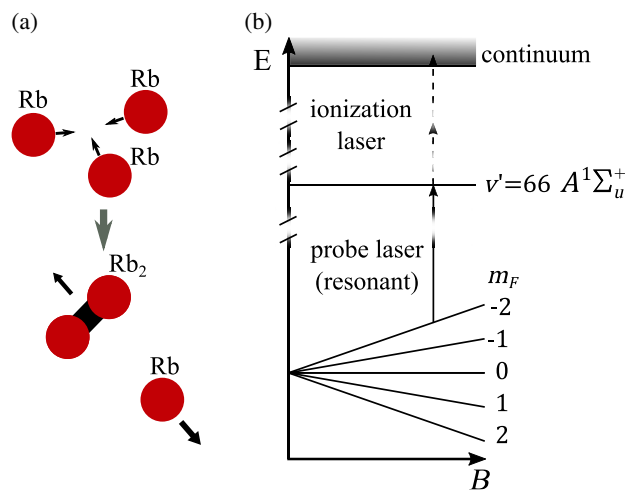

FIG. 1. (a) Three-body recombination of three neutral Rb atoms forming a Rb$_2$ dimer. (b) Schematic of the REMPI detection scheme, resolving the m_F quantum number of the molecule. As an example we consider here a molecular level manifold with $F = 2$. The linear Zeeman effect, due to a B field, splits the $F = 2$ levels into magnetic components $m_F = -2, -1, 0, 1, 2$. The splitting is large enough so that each level can be resolved via resonant excitation towards the intermediate level $v' = 66$, $A^1\Sigma_u^+$ with the probe laser. From there, two photons of the ionization laser ionize the molecule.

number of the total angular momentum F of the molecule excluding mechanical rotation and m_f is the magnetic quantum number of the total angular momentum f of the atom. The "no-spin flip" propensity rule indicates that the spectator atom participates in the reaction merely via mechanical forces; i.e., it can affect the rotational angular momentum of the forming molecule [19] but not its internal spin.

We carry out our experiments with an ultracold, thermal cloud of ^{87}Rb with a temperature of about 750 nK. The cloud consists of $N_{at} \approx 5 \times 10^6$ atoms which are trapped in a far-detuned, crossed optical dipole trap with a wavelength of about 1064 nm. The trapping frequencies are $\omega_{x,y,z} = 2\pi \times (23, 180, 178)$ Hz, where z represents the vertical direction. The atoms are in the electronic ground state and are initially spin polarized in the hyperfine state $f = 1, m_f = -1$. From this state also other m_f spin polarizations can be prepared.

Within the atomic gas, three-body recombination produces weakly bound Rb$_2$ molecules in the coupled $X^1\Sigma_g^+ - a^3\Sigma_u^+$ potentials. Given the initial peak particle density $n_0 \approx 0.9 \times 10^{14}$ cm^{-3} and a three-body recombination loss rate constant of $L_3 = (4.3 \pm 1.8) \times 10^{-29}$ cm^6 s^{-1} [27], about 1.5×10^5 atoms are lost due to three-body recombination in the first 500 ms. The molecular products are distributed over a range of different states, characterized by sets of vibrational, rotational, various spin and magnetic quantum numbers. We state-selectively probe the molecular products via resonance-enhanced multiphoton ionization (REMPI), followed by ion detection, similarly as in [19]. Figure 1(b) shows our REMPI scheme. The probe laser resonantly drives a transition to an intermediate level, which is located in the electronic state $A^1\Sigma_u^+$, has vibrational quantum number $v' = 66$ and a total angular momentum (excluding nuclear spin) J'. Hyperfine splittings of this excited level are negligibly small (< 3 MHz), such that the J' states form a simple rotational ladder with rotational constant $b_{v'} = 443$ MHz [28,29]. From the intermediate level, another two photons of the ionization laser ionize the molecule. We use the dipole trap laser as ionization laser. Its optical frequency is about 281.62915(6) THz. The probe laser and the dipole trap laser are wave meter locked with a precision of a few MHz. The probe laser intensity is ≈ 3 W cm^{-2} at the location of the atoms. This is sufficient to excite the probed molecules with high probability to the intermediate $A^1\Sigma_u^+$ level.

The ion detection works as follows. Directly after its ionization the molecule is trapped in a Paul trap [30] which is centered on the atomic cloud. Subsequently, the micromotion-driven ion elastically collides with ultracold atoms [19,32]. This leads to loss of atoms from the shallow dipole trap which is measured by absorption imaging. The losses increase with the number of trapped ions.

In order to spectrally resolve different m_F quantum numbers we apply a magnetic B field of several G to induce
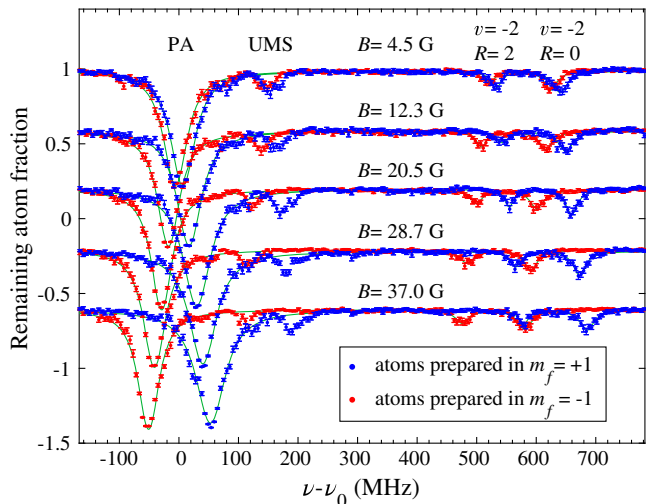

FIG. 2. REMPI spectra for experiments where the atomic sample is initially prepared in the magnetic spin state $m_f = -1$ (red data) or $m_f = +1$ (blue data) for different magnetic fields B. Shown is the remaining atom fraction as a function of the probe laser frequency ν. $\nu_0 = 281445.07(6)$ GHz. Nominally the remaining atom fraction can range between 1 and 0, but in order to improve visibility data sets for different magnetic fields are offset relative to each other in vertical direction. The loss signals for $v = -2, R = 0$ and $v = -2, R = 2$ product molecules, the photoassociation line (PA), and unidentified molecular bound states (UMS) are labeled. The green lines are fits according to Eq. (1) to the resonances.

linear Zeeman splitting. As an example, Fig. 1(b) shows the splitting of a $F = 2$ molecular bound state. In principle, $\vec{F}$ and the molecular rotation $\vec{R}$ couple to form the total angular momentum $\vec{F}_{tot}$. However, for the bound states considered here, this coupling is quite weak, corresponding to splittings between different F_{tot} levels smaller than 1 MHz [19]. Therefore, already the B field of several G efficiently decouples $\vec{F}$ and $\vec{R}$. A level for given m_F and R quantum numbers is then essentially $(2R + 1)$-fold energetically degenerate, according to the manifold of the m_R substates.

Figure 2 shows several measured REMPI spectra as a function of the probe laser frequency ν. The atoms of the cloud have initially been prepared either in state $m_f = -1$ (red data) or in state $m_f = +1$ (blue data). The measurements are carried out for various homogeneous magnetic fields in a range between 4.5 and 37.0 G. REMPI is carried out by switching on the probe laser for 500 ms. Afterwards, the magnetic field is turned off. We measure the remaining atom number 160 ms after the probe laser has been switched off, so that ions produced near the end of the REMPI period can still lead to atom losses. After normalization with the remaining atom number from an experiment where we work with a far off-resonant probe laser we obtain the remaining atom fraction, as shown in Fig. 2.

We first discuss the data set for $m_f = -1$ and the lowest magnetic field of 4.5 G. The strong resonance line at

$\nu - \nu_0 \approx 0$ is a photoassociation (PA) signal, where two $f = 1, m_f = -1$ atoms, which collide in an s-wave, form a molecule in state $v' = 66, A^1\Sigma_u^+$ with $J' = 1$. The observed width of the PA line is larger than the natural linewidth of about 12 MHz (FWHM) of the excited level due to saturation effects caused by atom loss.

We now focus on the loss signals about 520 and 640 MHz above the photoassociation line, which correspond to $v = -2, R = 2$ and $v = -2, R = 0$ product molecules, respectively. Here, v is the vibrational quantum number and R is the rotational quantum number. v is counted downwards starting from $v = -1$ for the most weakly bound vibrational state correlated to the atomic $f = 1$, $f = 1$ asymptote [33]. The $v = -2, R = 0$, 2 molecular products have been detected and identified in previous work of ours [19]. Their F quantum number is $F = 2$. Figure 2 shows that their resonance lines shift towards lower probe laser frequencies when increasing the magnetic field B, in parallel to the photoassociation line. Furthermore, we note that the depths and the widths of the lines stay the same when the B field is changed. This suggests that the molecules are produced in a particular m_F state, not a mix. We observe a very similar behavior when we switch to experiments with $f = 1, m_f = +1$ atoms [35] (blue data). Now, however, all lines shift in opposite direction as compared to the $f = 1, m_f = -1$ data. The observed linewidths are 30 ± 10 MHz (FWHM), which is a factor of 2 to 3 larger than the natural linewidth. The increased width can be explained as the result of several factors, such as the laser linewidth, a Doppler shift of the moving Rb$_2$ molecules, and saturation effects. We note that besides the already discussed lines in Fig. 2, there are two additional lines (at around $\nu - \nu_0 = 90$ and 140 MHz for the data sets at $B = 4.5$ G). These belong to so far unidentified molecular bound states (UMS), which are detected through a different intermediate state [19].

We now carry out a more quantitative analysis of the Zeeman energy level shifts. Since the excited $v' = 66$, $A^1\Sigma_u^+$ level is essentially insensitive to applied magnetic fields, the observed line shifts in Fig. 2 correspond directly to the Zeeman shifts of the atomic states or the molecular product states. In order to determine the center position ν_i of each observed resonance line i we fit the function

$$N(\nu)/N_0 = \exp\left(\sum_i \frac{-A_i}{(\nu - \nu_i)^2 + (\Gamma_i/2)^2}\right) \quad (1)$$

to the data of the remaining atom fraction, $N(\nu)/N_0$. Here, A_i is an amplitude, and Γ_i is the linewidth. The results are presented in Fig. 3, together with additional REMPI data beyond the frequency range shown in Fig. 2. The additional data correspond to transitions from $v = -2, R = 2$, and $R = 4$ towards $J' = 3$ of $v' = 66, A^1\Sigma_u^+$ [37]. Together with these, our study covers all possible [38] rotational product states $R = 0, 2, 4$ of the $v = -2$ state. Figure 3 shows that the
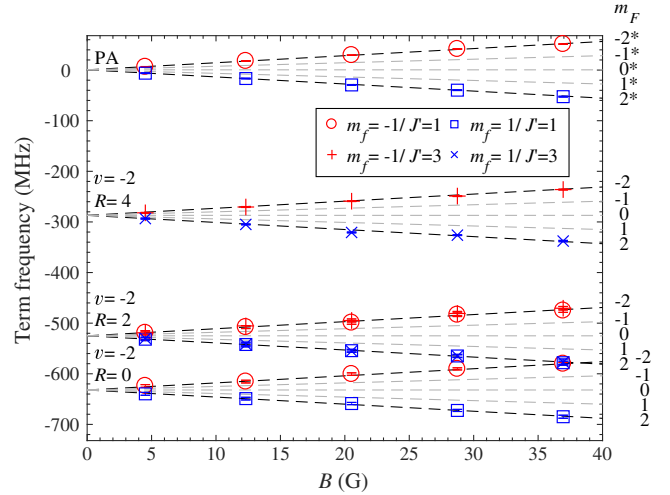

FIG. 3. Zeeman shifts. Shown are the term frequencies (i.e., negative laser frequency positions relative to the threshold at $B = 0$) of the two-atom scattering states (PA) and the molecular levels $v = -2, R = 0, 2, 4$ as a function of the magnetic field B. For each plot symbol the legend indicates in which spin polarization the atomic cloud has been prepared, and which J' level is addressed in the REMPI measurement. The error bars correspond to the 95% confidence intervals of the fits according to Eq (1). The dashed lines are calculations. The asterisk (*) next to a m_F quantum number marks a two-atom scattering state.

$J' = 1$ and $J' = 3$ data sets for the $v = -2$, $R = 2$ state lie precisely on top of each other, as required by consistency.

Next, we compare the measured energy positions of the product molecule levels to calculated Zeeman level positions (dashed lines). Since the molecules are extremely weakly bound, their magnetic moment is essentially equal to the sum of the magnetic moments of the free atoms a, b. In the limit of the linear Zeeman effect, the energy level positions are then given by $E_b + g_f\mu_B(m_{f,a} + m_{f,b})B$, where E_b is the binding energy of the respective state at zero field, μ_B is Bohr's magneton, $g_f = -1/2$ is the g-factor, and $m_{f,a/b}$ is the magnetic quantum number of atom a or b, respectively. Figure 3 clearly shows that three-body recombination produces $m_F = +2$ molecules in an ensemble of $m_f = +1$ atoms and it produces $m_F = -2$ molecules in an ensemble of $m_f = -1$ atoms. Apparently, the total magnetic quantum number $m_F = m_{f,a} + m_{f,b}$ of the two atoms forming the molecule is conserved in three-body recombination. This goes well along with a propensity rule for the conservation of the F quantum number and the parity, observed in our previous work [19].

Finally, we investigate molecular products in an atomic sample consisting of a mix of m_f states which has been produced by ramping the B field through zero field. Figure 4 shows a REMPI spectrum for $B = 37$ G. As expected, the photoassociation signal around ν_0 is now a multiline structure involving all m_F components $-2, -1, 0$, 1, 2 resulting from all pair combinations of $m_f = -1, 0, 1$
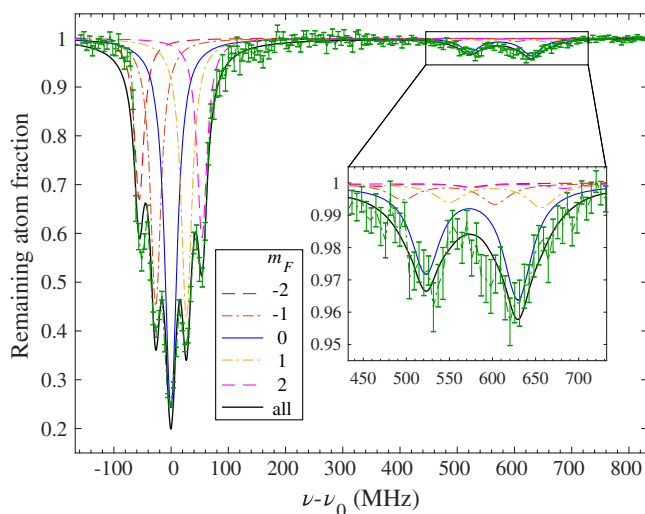
FIG. 4. REMPI spectrum for an initial cloud of atoms prepared in a mix of m_f quantum numbers at a magnetic field $B = 37$ G. The strong multiline signal at $\nu - \nu_0 \approx 0$ corresponds to photoassociation. The signal is decomposed into the different m_F components for atom pairs using Eq. (1). The inset is an enlargement of the $v = -2, R = 0$ and $v = -2, R = 2$ molecular signals. Here, the dashed and solid colored lines correspond to calculations for the individual molecular m_F populations, which are formed in three-body recombination. The black solid line is the sum of these populations.

atoms. The $v = -2, R = 0, 2$ molecular signal between 450 MHz and 700 MHz (inset is an enlargement) is now a broad double dip as a result of the ten overlapping molecular signals corresponding to the different combinations of R and m_F quantum numbers. Since no further substructure is observable, a direct decomposition into molecular subcomponents is problematic. Therefore, we choose the following way for the analysis of the molecular signal. We first determine the three m_f populations of the initial atom cloud, and with these we predict the $v = -2, R, m_F$ populations of the molecules and the corresponding spectrum, which can be compared to the measurements. From additional photoassociation loss measurements, which are carried out without ion trap and a simple photoassociation model which assumes the same photoassociation efficiency for all $m_F = m_{f,a} + m_{f,b}$ atom pairs, we extract the following m_f distribution: 25%, 45%, 30% for $m_f = -1, 0, 1$, respectively. Using this, we predict the three-body recombination product molecule distribution to be 9%, 17%, 41%, 20%, 13% for $m_F = -2, -1, 0, 1,$ 2, respectively. Here, we use that the m_F quantum number is conserved for three-body recombination and assume that the three-body recombination rate constant is identical for the different m_F channels. The corresponding calculated m_F signals are shown in the inset of Fig. 4, using individual linewidths of 40 MHz. The black line which is the sum over all signals agrees quite well with the experimentally observed double-dip structure.

In conclusion, we have carried out state-to-state measurements for three-body recombination with neutral ^{87}Rb atoms in the regime of non-resonant two-particle interactions. We have demonstrated spectroscopic resolution of the m_F magnetic quantum states of the product molecules, in addition to the previously resolved vibrational, rotational, hyperfine degrees of freedom. Our studies suggest the propensity rule that the m_F quantum number is conserved when forming weakly bound Rb$_2$ molecules via three-body recombination of cold ^{87}Rb atoms.

For the future, we plan to probe more deeply bound molecular states in order to investigate whether this and the previously found propensity rules change, as indicated by our earlier work [18]. From such experiments we can possibly gain information on how much the short range details of the interaction potentials influence the product distribution. Furthermore, it will be interesting to test whether the propensity rules found for ^{87}Rb break down for other atomic species. ^{87}Rb is special since its triplet and singlet scattering lengths are almost identical. Finally, we plan to further extend the detection method to also resolve the magnetic quantum numbers m_R of molecular mechanical rotation, as this would complete the experimental method for determining all internal quantum numbers of the molecule for the case that $\vec{R}$ and $\vec{F}$ are decoupled.

[1] D. Nesbitt, Chem. Rev. **112**, 5062 (2012).

[2] X. Yang, Annu. Rev. Phys. Chem. **58**, 433 (2007).

[3] H. Pan, K. Liu, A. Caracciolo, and P. Casavecchia, Chem. Soc. Rev. **46**, 7517 (2017).

[4] J. Jankunas and A. Osterwalder, Annu. Rev. Phys. Chem. **66**, 241 (2015).

[5] S. Y. T. van de Meerakker, H. L. Bethlem, N. Vanhaecke, and G. Meijer, Chem. Rev. **112**, 4828 (2012).

[6] J. L. Bohn, A. M. Rey, and J. Ye, Science **357**, 1002 (2017).

[7] G. Quéméner and P. S. Julienne, Chem. Rev. **112**, 4949 (2012).

[8] N. Balakrishnan, J. Chem. Phys. **145**, 150901 (2016).

[9] R. V. Krems, Phys. Chem. Chem. Phys. **10**, 4079 (2008).

[10] L. D. Carr, D. DeMille, R. V. Krems, and J. Ye, New J. Phys. **11**, 055049 (2009).

[11] J. Doyle, B. Friedrich, R. V. Krems, and F. Masnou-Seeuws, Eur. Phys. J. D **31**, 149 (2004).

[12] V. Aquilanti, M. Bartolomei, F. Pirani, D. Cappelletti, F. Vecchiocattivi, Y. Shimizu, and T. Kasai, Phys. Chem. Chem. Phys. **7,** 291 (2005).

[13] H. Ohoyama, K. Yasuda, and T. Kasai, J. Phys. Chem. A **113,** 14785 (2009).

[14] M. H. G. de Miranda, A. Chotia, B. Neyenhuis, D. Wang, G. Quéméner, S. Ospelkaus, J. L. Bohn, J.Ye, and D. S. Jin, Nat. Phys. **7,** 502 (2011).

[15] S. D. S. Gordon, J. J. Omiste, J. Zou, S. Tanteri, P. Brumer, and A. Osterwalder, Nat. Chem. **10,** 1190 (2018).

[16] A. Mattheus, A. Fischer, G. Ziegler, E. Gottwald, and K. Bergmann, Phys. Rev. Lett. **56,** 712 (1986).

[17] W. E. Perreault, N. Mukherjee, and R. N. Zare, Science **358,** 356 (2017).

[18] A. Härter, A. Krükow, M. Deiß, B. Drews, E. Tiemann, and J. Hecker Denschlag, Nat. Phys. **9,** 512 (2013).

[19] J. Wolf, M. Deiß, A. Krükow, E. Tiemann, B. P. Ruzic, Y. Wang, J. P. D'Incao, P. S. Julienne, and J. Hecker Denschlag, Science **358,** 921 (2017).

[20] C. Chin, R. Grimm, P. Julienne, and E. Tiesinga, Rev. Mod. Phys. **82,** 1225 (2010).

[21] J. Rui, H. Yang, L. Liu, D.-C. Zhang, Y.-X. Liu, J. Nan, Y.-A. Chen, B. Zhao, and J.-W. Pan, Nat. Phys. **13,** 699 (2017).

[22] S. Knoop, F. Ferlaino, M. Berninger, M. Mark, H.-C. Nägerl, R. Grimm, J. P. D'Incao, and B. D. Esry, Phys. Rev. Lett. **104,** 053201 (2010).

[23] D. K. Hoffmann, T. Paintner, W. Limmer, D. S. Petrov, and J. Hecker Denschlag, Nat. Commun. **9,** 5244 (2018).

[24] F. Ferlaino, A. Zenesini, M. Berninger, B. Huang, H.-C. Nägerl, and R. Grimm, Few-Body Syst. **51,** 113 (2011).

[25] K. M. Jones, E. Tiesinga, P. D. Lett, and P. S. Julienne, Rev. Mod. Phys. **78,** 483 (2006).

[26] M. McDonald, I. Majewska, C.-H. Lee, S. S. Kondov, B. H. McGuyer, R. Moszynski, and T. Zelevinsky, Phys. Rev. Lett. **120,** 033201 (2018).

[27] E. A. Burt, R. W. Ghrist, C. J. Myatt, M. J. Holland, E. A. Cornell, and C. E. Wieman, Phys. Rev. Lett. **79,** 337 (1997).

[28] M. Deiß, B. Drews, J. Hecker Denschlag, and E. Tiemann, New J. Phys. **17,** 083032 (2015).

[29] A. N. Drozdova, A. V. Stolyarov, M. Tamanis, R. Ferber, P. Crozet, and A. J. Ross, Phys. Rev. A **88,** 022504 (2013).

[30] For a detailed description of the setup of the nested atom and ion traps, see Ref. [31].

[31] S. Schmid, A. Härter, A. Frisch, S. Hoinka, and J. Hecker Denschlag, Rev. Sci. Instrum. **83,** 053108 (2012).

[32] A. Härter, A. Krükow, A. Brunner, and J. Hecker Denschlag, Appl. Phys. Lett. **102,** 221115 (2013).

[33] Detailed information on the $X^1\Sigma_g^+ - a^3\Sigma_u^+$ level structure can be found, e.g., in Refs. [19,34].

[34] C. Strauss, T. Takekoshi, F. Lang, K. Winkler, R. Grimm, J. Hecker Denschlag, and E. Tiemann, Phys. Rev. A **82,** 052514 (2010).

[35] To prepare $m_f = +1$ atoms, we start with a cloud of $m_f = -1$ atoms at a small bias magnetic field of $B = 4.5$ G and suddenly reverse the magnetic field direction, which flips the quantization axis, but the spins cannot follow [36]. The resulting $f = 1, m_f = +1$ population is 95% pure.

[36] T. Volz, S. Dürr, S. Ernst, A. Marte, and G. Rempe, Phys. Rev. A **68,** 010702(R) (2003).

[37] For a rotational quantum number R of the weakly bound ground state Rb_2 molecule the selection rules for electric dipole transitions allow for $R \to J' = +1$ for $R = 0$, and $R \to J' = R \pm 1$, otherwise.

[38] According to the propensity rule from Ref. [19] dominantly weakly bound product states with positive parity, i.e., even R, are produced in our experiment. Furthermore, for the $v = -2$ state, $R = 4$ is the last rotational bound state below the scattering asymptote.